

## **Biodistribution and racemization of gut-absorbed L/D-alanine in germ-free mice**

Tian (Autumn) Qiu<sup>1,2,#</sup>, Cindy J. Lee<sup>1</sup>, Chen Huang<sup>3</sup>, Dongkyu Lee<sup>1,\*</sup>, Stanislav S. Rubakhin<sup>1,2,3</sup>,  
Jonathan V. Sweedler<sup>1,2,3</sup>

<sup>1</sup>Department of Chemistry, University of Illinois, Urbana-Champaign, Urbana, IL 61801

<sup>2</sup>Beckman Institute, University of Illinois, Urbana-Champaign, Urbana, IL 61801

<sup>3</sup>Neuroscience Program, University of Illinois, Urbana-Champaign, Urbana, IL 61801

\* Current address: College of Pharmacy, Chung-Ang University, Seoul, 06974, Republic of Korea

# Current address: Department of Chemistry, Michigan State University, East Lansing, MI 48824

E-mail address of the corresponding author: [jsweedle@illinois.edu](mailto:jsweedle@illinois.edu)

**Keywords:** amino acids, NMDAR, microbiome, mouse, mass spectrometry

**Running title:** Biodistribution and racemization of gut-absorbed L/D-alanine.

## Abstract

Discovery and characterization of microbiome-derived metabolites are important for characterization of the different functional systems including the microbiome-gut-brain axis and for discovery of new disease treatments. Essential to microorganisms, D-Alanine (D-Ala) is found in many animals and acts as a potent co-agonist of the *N*-methyl-D-aspartate receptors (NMDAR). These receptors are widely expressed and have a variety of functions in the nervous and endocrine systems. The gut microbiome, diet and putative endogenous synthesis are the potential sources of D-Ala in animals. Understanding the sources of D-Ala and distribution of gut-absorbed D-Ala in mammals is critical for the evaluation of interaction between an animal and its microbiota. In this work, we used germ-free mice fed with stable isotope-labeled L-/D-Ala to study the biodistribution of gut-absorbed D-Ala without interference from microbiota. This also allows the determination of endogenous D-Ala synthesis through enantiomeric conversion. D-Ala is absorbed by both the small intestines and colon; the distribution of gut-absorbed D-Ala is related to the tissue type and treatment time (1-hour and 2-week). The highest levels of D-Ala accumulate in the pancreatic islets and acinar tissues followed by the brain and pituitary gland. Changes in tissue peptide profiles measured after 2-weeks of D-Ala treatment suggest that D-Ala impacts the activity of the hypothalamus-pituitary-adrenal axis. No endogenous synthesis of D-Ala via racemization was reliably observed in germ-free mice. Alanine racemization was readily observed in bacterial culture and regular mice possessing normal microbiota supporting the idea that mice lack a functional alanine racemase enzyme.

## Introduction

Investigation of chemical interactions in the microbiota-gut-brain axis has become an increasingly important for the understanding and treatment of neurological diseases such as autism spectrum disorder (1), Alzheimer's disease (2), and Parkinson's disease (3). The microbiome-derived metabolites can be involved in cell-cell chemical signaling in different tissues and organs of the host including the endocrine and central nervous system (CNS). The gut microbiome is known a source of a variety of bioactive molecules such as trimethylamine-N-oxide linked to cardiovascular health (4), phenolic metabolites that reduce neurodegeneration (5), short-chain fatty acids (SCFAs) related to metabolic diseases (6), and neurotransmitters such as  $\gamma$ -aminobutyric acid (GABA) that can regulate the enteric nervous systems (ENS) (7). Discovery and characterization of functional microbiome-derived metabolites is thus important for future microbiome-based disease interventions.

D-Alanine (D-Ala) is a poorly characterized but intriguing potential microbial signaling molecule in the microbiome-gut-brain axis. D-Ala is an essential component of the bacterial cell walls, produced from L-Ala by microbial alanine racemases and exists almost ubiquitously in the realm of microorganisms (8). Like D-serine (D-Ser), D-Ala interacts with the glycine binding site of the N-methyl-D-aspartate receptors (NMDARs). NMDAR is an ionotropic glutamate receptor expressed in different cell types including the neurons where it is mainly associated with excitatory synapses (9). D-Ser modulates NMDAR activity in the CNS thus impacts brain functions demonstrating clinical relevance to neurological disorders such as depression and schizophrenia (10–12). Similarly, D-Ala has been shown to be a potent, stereo-selective co-agonist of NMDAR *in vitro* (13, 14). Although *in vivo* evidence of D-Ala function is currently lacking and under investigation, evidence suggests D-Ala may be a potential biomarker involved in a range of functions, particularly in the nervous and endocrine systems. As examples, D-Ala levels fluctuate in a circadian manner in both rodents and human tissues (15–18). As with several other D-amino acids, D-Ala is detected in endocrine structures including the insulin-secreting  $\beta$ -cells in the pancreatic islets and adrenocorticotrophic hormone (ACTH)-secreting cells in the pituitary gland (19–22). Therefore, modulation of D-Ala of activity of the hypothalamus-pituitary-adrenal (HPA) axis and pancreatic islets *in vivo* is hypothesized. In addition, changed D-Ala levels were found in samples from individuals with various diseases such as Alzheimer's disease, diabetes, renal diseases, cancers, and more, as summarized in our previous review (23). This makes D-Ala as a potential biomarker and pharmacological target for these diseases.

Surprising given this interest, the origin of the of D-Ala in animals, particularly in the widely used rodents, is not known. There are several potential sources of D-Ala in animals – diet, the gut microbiota, and endogenous synthesis. Diet, especially fermented and processed food, contains D-Ala, thus being a source of D-Ala (24). Microbial origin of D-Ala is supported by a number of evidence including results of our work showing D-Ala production by isolated gut microbial species (25), demonstration of endogenous alanine racemases expression in microorganisms (26, 27), and dependence of D-Ala levels on the presence of the gut microbiota (17). Although no endogenous alanine racemases have been identified in mammals, an interesting hypothesis focuses on the potential source of D-Ala in saliva and salivary glands (28, 29). These three factors – diet, gut microbiota, and hypothetical endogenous synthesis – are intertwined, making it hard to differentiate the origins of D-Ala in animal tissues and organs.

In this study, we utilized the germ-free and regular mice orally fed with stable both isotopically labeled D/L-Ala. Main goals of the study are to: 1) identify the origins of D-Ala in mouse, 2) track gut-absorbed D-Ala biodistribution, and 3) provide information on the biological functions of D-Ala (**Figure 1**). The utilization of germ-free mice eliminated microbiota as a source of D-Ala including related bacterial alanine racemase activity. Stable isotope labeled Ala provided direct evidence of D-Ala gut absorption and biodistribution as well as absence of endogenous L-Ala racemization in our experimental time frame. In the experiments, solutions containing D- or L-Ala were orally administered via one-time gavage (1-hour exposure) or by supplementing drinking water with these isotopes for two weeks. These two experimental scenarios explore the correlation of the metabolite's biodistribution to short- and long-term exposures of animals to exogenous L/D-Ala. To explore the potential endogenous synthesis of D-Ala via racemization, stable isotope labeled L-Ala was fed to germ-free and regular mice and the D-Ala isotope product was monitored. Chiral derivatization of amino acids using a modified version of Marfey's reagents was used to separate the D-/L-Ala enantiomers extracted from samples. Concentrations of unlabeled and isotope-labeled Ala were measured using an ultra-performance liquid chromatography (UPLC) coupled to a triple quadrupole mass spectrometer (TQMS). Peptide profiles in islets and pituitary gland were characterized by a matrix-assisted laser desorption/ionization (MALDI) time-of-flight (TOF) mass spectrometer. For the first time, we identify the sources of D-Ala in mammals and reveal the biodistribution of D-Ala through gut absorption, paving the ways for future functional studies of this potential signaling molecule in the microbiome-gut-brain axis.

## Results

### Differential sample-specific levels of endogenous L/D-Ala in mouse food, germ-free and regular mice

Analytical measurements of endogenous, unlabeled D- and L-Ala were performed in the animal samples as well as mouse chow (**Figure 2**). D-Ala percentages ( $\text{D-Ala}/(\text{L-Ala}+\text{D-Ala})\%$ ) for animal samples (**Figure 2(a)**) and mouse chow (**Figure 2(b)**) were calculated, and plotted together with D-Ala concentrations (**Figure 2(c)(d)(e)**). To compare D-Ala% and D-Ala levels in each type of sample, pairwise comparisons were individually performed between germ-free and regular mice. Parametric Welch's t-tests were implemented initially because of unequal variances; however, non-parametric Mann-Whitney tests with less assumptions were chosen due to the small degree of freedoms in Welch's t-tests that result from the small sample sizes ( $n=3-8$ ). Statistical significance was set at  $\alpha=0.05$ . We found that the plasma, pituitary, salivary gland, small intestine content, colon, and colon content showed higher D-Ala% in regular mice compared to germ-free mice. However, the trends for D-Ala concentration in samples were not always consistent with D-Ala%. Only acinar tissues, colon, and gut contents showed higher D-Ala concentrations. Among all samples, colon contents from regular mice showed the highest D-Ala%. Pancreatic islets and acinar tissues were among the highest in the measured tissue types in both germ-free and regular mice. While islets and acinar tissues showed similar D-Ala% in germ-free and regular mice, acinar tissues in both mouse type showed higher D-Ala concentrations. Interestingly, the D-Ala concentration in regular mice was significantly higher than that in germ-free mice while D-Ala% was similar, indicating a similar trend of L-Ala in the acinar tissues of regular mice.

## Biodistribution of gut-absorbed D-Ala-<sup>13</sup>C<sub>3</sub>,<sup>15</sup>N in germ-free mice

Two D-Ala-<sup>13</sup>C<sub>3</sub>,<sup>15</sup>N oral administration scenarios were implemented, a one-time gavage of ~40 mg with 1-hour waiting time and a two-week feeding of ~100 mg D-Ala-<sup>13</sup>C<sub>3</sub>,<sup>15</sup>N. D-Ala-<sup>13</sup>C<sub>3</sub>,<sup>15</sup>N levels in various samples were measured and calculated. The isotopic Ala levels were corrected for analytical and instrumental effects using isotopically labeled L-Ser and L-Leu as outlined in the methods and the following calculations involved these corrected levels. To enable comparisons across sample types, D-Ala-<sup>13</sup>C<sub>3</sub>,<sup>15</sup>N concentrations were divided by total unlabeled Ala in each sample, generating ratios of D-Ala-<sup>13</sup>C<sub>3</sub>,<sup>15</sup>N over total unlabeled Ala in the same sample (**Equation 1**):

$$\text{D - Ala isotope ratio} = \frac{[\text{D - Ala isotope}]}{[\text{total unlabeled Ala}] \text{ in the same sample}} \quad (1)$$

A visual comparison across different samples revealed that except for in the acinar tissues and islets, D-Ala-<sup>13</sup>C<sub>3</sub>,<sup>15</sup>N/Ala ratios in plasma were higher than most of the other samples (**Figure S1**). Pearson correlation showed that plasma D-Ala-<sup>13</sup>C<sub>3</sub>,<sup>15</sup>N ratios were positively correlated to those of most other samples (**Table S1**), indicating the level of D-Ala-<sup>13</sup>C<sub>3</sub>,<sup>15</sup>N in plasma can be representative of biological variations for mouse individuals. This finding together with the observed drastically different plasma levels of D-Ala-<sup>13</sup>C<sub>3</sub>,<sup>15</sup>N in gavage and feeding (**Figure 3(a)**) make it possible to normalize D-Ala-<sup>13</sup>C<sub>3</sub>,<sup>15</sup>N levels and thus allow comparisons between feeding scenarios and across sample types.

To enable comparison between two oral administration scenarios, D-Ala-<sup>13</sup>C<sub>3</sub>,<sup>15</sup>N concentrations in various tissues/gut content in their own metrics (pmole over mg tissues/mg feces/μg proteins) were divided by the plasma D-Ala-<sup>13</sup>C<sub>3</sub>,<sup>15</sup>N level (pmole/μL plasma) (**Equation 2**):

$$\text{Normalized D - Ala isotope concentration} = \frac{[\text{D - Ala isotope}]_{\text{tissue or gut contents}}}{[\text{D - Ala isotope}]_{\text{plasma}} \text{ of the same animal}} \quad (2)$$

Pairwise comparisons of such normalized D-Ala-<sup>13</sup>C<sub>3</sub>,<sup>15</sup>N concentration between gavage and feeding of the same sample type were performed using non-parametric Mann-Whitney tests due to the small sample sizes (**Figure 3(b)**). Statistical significance was set at significance level (α) of 0.05. Results showed that normalized D-Ala-<sup>13</sup>C<sub>3</sub>,<sup>15</sup>N concentrations in pituitary and brain were statistically significantly higher in the feeding group than in the gavage group, while interestingly, the small intestine contents showed lower normalized D-Ala-<sup>13</sup>C<sub>3</sub>,<sup>15</sup>N concentrations in the feeding group.

As D-Ala-<sup>13</sup>C<sub>3</sub>,<sup>15</sup>N concentrations in different sample types have different metrics, to enable comparisons among sample types, the unitless D-Ala isotope ratios (**Equation 1**) were calculated and further normalized to the plasma D-Ala-<sup>13</sup>C<sub>3</sub>,<sup>15</sup>N ratio to count for biological variations (**Equation 3; Figure 3(c)(d)**):

$$\text{Normalized D - Ala isotope ratio} = \frac{(\text{D - Ala isotope ratio})_{\text{tissue or gut contents}}}{(\text{D - Ala isotope ratio})_{\text{plasma}} \text{ of the same animal}} \quad (3)$$

After calculation of **Equation 3**, the normalized D-Ala-<sup>13</sup>C<sub>3</sub>,<sup>15</sup>N ratios in plasma samples equal to 1, shown as the dashed lines in **Figure 3(c)(d)**. It appears that in both gavage and feeding groups, islets and acinar tissues always showed similar or higher normalized D-Ala-<sup>13</sup>C<sub>3</sub>,<sup>15</sup>N

ratios than the plasma, while most of the other samples seem to have much lower ratio compared to plasma, except for the brain and pituitary samples from the feeding group. This is consistent with the results from normalized D-Ala-<sup>13</sup>C<sub>3</sub>,<sup>15</sup>N concentrations (**Figure 3(b)**). To determine the effect of sample type, a non-parametric Kruskal-Wallis ANOVA test plus post-hoc Dunn's multiple comparison was performed. ANOVA results showed that sample type had a statistically significant effect on the normalized D-Ala-<sup>13</sup>C<sub>3</sub>,<sup>15</sup>N ratio in both the gavage (p=0.0002) and the feeding groups (p=0.0001). Post hoc Dunn's multiple comparisons showed that in both the gavage and feeding groups, normalized D-Ala-<sup>13</sup>C<sub>3</sub>,<sup>15</sup>N ratios in islets and acinar tissues significantly contributed to the observed variances (**Figure 3(c)(d)**).

### **Differences in pancreatic islets and pituitary peptide profiles determined by MALDI-TOF MS analysis**

Peptides were also extracted from the same pancreatic islets and pituitary samples collected from germ-free mice fed with stable isotope-labeled L- and D-Ala solutions for two weeks. MALDI-TOF mass spectrometer was used to semi-quantitatively profile peptide level changes in treated groups. Mass lists were built using acquired data and information on analytes reported by peptidomics studies of the pancreatic islets and pituitaries (30–34), plus unknown m/z values detected in our samples (at least in 10 out of 12 samples). A detailed mass list can be found in the **Supporting Information**. The volcano plots in **Figure 4** show the differences in peptide profiles of the pancreatic islets and pituitary after the 2-week addition of stable isotope labeled L- and D-Ala into drinking water. Borderlines for log<sub>2</sub> (fold change) were drawn at -1 and 1 and for p-values were placed at -log(0.05). Individual t-tests were used to compare the normalized, log<sub>2</sub>-transformed levels of putative peptide signals in control and treated groups. Potential false discoveries should be kept in mind as no multiplicity was corrected. In general, treatments with stable isotope labeled L- and D-Ala resulted in recognizable differences in peptide profiles of both the pancreatic islets and pituitary. After D-Ala-<sup>13</sup>C<sub>3</sub>,<sup>15</sup>N treatment, islets showed statistically significant increased intensity of signal at m/z 1952 (matching mouse insulin 1 fragment 61-79) and decrease of signal at m/z 3919.1 (unknown) (**Figure 4(a)**). Larger-than-2-fold but not statistically significantly lower insulin signal at m/z 5797.5 was also observed. No similar changes were found in L-Ala-treated groups of pancreatic islets (**Figure 4(b)**). For pituitary, we observed some similar trends in both groups treated with stable isotope-labeled L- and D-Ala, including m/z 2528.4 (unknown), 3059.7 (unknown), 2922.6 (unknown), 4437.5 (matching γ-LPH). Unique features for D-Ala-<sup>13</sup>C<sub>3</sub>,<sup>15</sup>N treatment were shown at m/z 1983.0 (unknown) and m/z 2586.3 (matching phosphorylated CLIP).

### **Evaluation of alanine racemase activity in bacterial culture, regular, and germ-free mice**

Alanine racemase activity can be detected by monitoring conversion from L-Ala-2,3,3,3-d<sub>4</sub> to D-Ala-3,3,3,3-d<sub>3</sub> (**Figure 5(a)**). D-Ala-3,3,3,3-d<sub>3</sub> levels in different samples collected from germ-free mice, regular mice, and bacterial culture after administration of L-Ala-2,3,3,3-d<sub>4</sub> were determined from monitoring signals in MRM channels for D-Ala-3,3,3,3-d<sub>3</sub> and shown in **Figure 5** after calculations from raw signals to final concentrations. In all animal samples, we observed background signals in the MRM channels for D-Ala-3,3,3,3-d<sub>3</sub> surrounding the retention time of D-Ala (**Figure S2** as an example), which we believe were from the biological matrices and thus result in the trace levels of D-Ala-3,3,3,3-d<sub>3</sub> shown in control samples (gray bars in **Figure 5**).

Pairwise comparisons between control and treated groups were performed using non-parametric Mann-Whitney tests. No statistically significant differences in D-Ala-3,3,3-d<sub>3</sub> levels found between control animals and mice fed with L-Ala-2,3,3,3-d<sub>4</sub> for 2 weeks, indicating no alanine racemase activities detected in germ-free mice fed with L-Ala-2,3,3,3-d<sub>4</sub> for two consecutive weeks.

To investigate alanine racemase activity in pure *E. coli* culture, L-Ala-2,3,3,3-d<sub>4</sub> was supplemented into culture media and D-Ala-3,3,3-d<sub>3</sub> concentrations in the bacterial biomass were determined. Results showed alanine racemase activities in *E. coli* biomass 1 h and 5 h incubations leading to time-dependent increase in levels of D-Ala enantiomer (**Figure 5(f)**). Although germ-free mice did not show detectable alanine racemase activities, the transformation of L-Ala-2,3,3,3-d<sub>4</sub> to D-Ala-3,3,3-d<sub>3</sub> were detected in regular mice only 1-hour after oral gavage of a single high dose of L-Ala-2,3,3,3-d<sub>4</sub> (**Figure 5(g)(h)(i)(j)**). The patterns of normalized D-Ala-3,3,3-d<sub>3</sub> ratios (**Equation 3**) across sample types were similar to those from gavage experiments of D-Ala-<sup>13</sup>C<sub>3</sub>,<sup>15</sup>N (**Figure S3, Figure 3(c)**), except for in colon and colon contents. Unlike results from gavage experiments with germ-free mice, normalized D-Ala-3,3,3-d<sub>3</sub> ratios in colon and colon contents were comparable to that in the plasma of regular mice after L-Ala-2,3,3,3-d<sub>4</sub> gavage, indicating microbial racemase activities in the colon content.

## Discussion

Using germ-free mice and stable isotopically labeled alanine for oral administration, our results have several major conclusions. First, the D-Ala in mouse originates from both food and microbiota, but not endogenous synthesis. Germ-free mice have detectable levels of D-Ala, indicating that there are sources of D-Ala that are not related to microbiota (**Figure 2(a)**). As the mouse chow has high D-Ala%, food can be a source of D-Ala (**Figure 2(b)**). Many studies have shown that both raw and processed food contain various levels of D-AAAs, including D-Ala (35). Comparison between germ-free and regular mice clearly shows that the existence of microbiota drastically increases the D-Ala levels in colon contents and colon tissue, indicating microbiota-derived D-Ala may be absorbed through the colon (**Figure 2(a)(c)(e)**). D-Ala% in the plasma, pituitary, salivary glands, and small intestine contents are higher in regular mice compared to those in germ-free mice, although the differences are less obvious or disappeared when looking at D-Ala concentrations (**Figure 2(a)(c)**). For plasma, pituitary and pancreas, we did not see as drastic differences in germ-free compared to specific-pathogen free mice as reported by Karawaka, et al (17). This could be due to reasons including different animal strains, food of choice, D-Ala analysis measurement techniques, sample type (e.g., entire pancreas vs. isolated acinar tissues), extent of blood removal during sample preparation, etc. For example, Bruckner et al. determined the percentage of D-Ala in rat chow as high as 6.9% (36), and we measured 12.6% in the mice chow used in our study. Interestingly, the D-Ala levels we measured in this study seem to be among the lowest reported except for in colon contents (**Table S2**).

Our results showed that there was no detectable alanine racemase activity in germ-free mice. Alanine racemases, which convert L-Ala to its D-form, have been found in many microbes and several aquatic invertebrates, but no alanine racemase has been characterized in vertebrates (8, 23). Some evidence of endogenous alanine racemase activity in vertebrates relate to saliva and salivary glands. More than 30% of total Ala has been reported to be in D-form in human saliva (28, 37). However, the same studies showed that the D-Ala% were lower in oral tissue

cells and in salivary glands, while microorganisms in the oral cavity showed a higher percentage of D-Ala. Low levels of D-Ala were also observed in the rat salivary glands (0.2-0.3%) (29). These suggest that D-Ala originating from the oral microbiome contributing to the D-Ala detected in saliva. Nevertheless, the hypothesis of D-Ala endogenous synthesis cannot be ruled out. Our results clearly showed that after 2-week oral administration of L-Ala-2,3,3,3-d<sub>4</sub>, no L- to D-Ala transformation was observed (**Figure 5(b-e)**). We conclude that no endogenous alanine racemase activities are present in germ-free mice within the timeframe and the treatment dose we evaluated. As microbes can rapidly transform L-Ala-2,3,3,3-d<sub>4</sub> to its D-form (**Figure 5(f)**), it was not surprising that a short gavage experiment of L-Ala-2,3,3,3-d<sub>4</sub> performed with regular mice possessing normal microbiota resulted in detection of alanine racemase activity in all sample types examined (**Figure 5(g-j)**). In fact, the comparison of normalized D-isotope ratio to unlabeled Ala across sample types showed very similar patterns to those observed in the gavage experiment involving D-Ala-<sup>13</sup>C<sub>3</sub>, <sup>15</sup>N (**Figure S3; Figure 3(c)**), except for the colon and colon contents, where D-Ala was produced by microbial alanine racemase activities. Our results strongly support the conclusions that the D-Ala in mouse originated from the microbiota and food, and not by endogenous biosynthesis through enzymatic racemization.

We demonstrated that D-Ala can be absorbed by the intestines and showed the biodistribution of gut-absorbed D-Ala using D-Ala-<sup>13</sup>C<sub>3</sub>, <sup>15</sup>N oral administration in germ-free mice without interference from microbiota. Oral administration of D-Ala in rodents has been done (38–41), showing increased levels of D-Ala in serum, urine, and some parts of the brain, but not pituitary. However, the D-Ala formed from alanine racemase activity from the gut microbiota may have hampered an accurate evaluation of the gut-absorbed D-Ala biodistribution. With germ-free mice and D-Ala-<sup>13</sup>C<sub>3</sub>, <sup>15</sup>N, we differentiated the exogenous D-Ala through oral administration and the unlabeled D-Ala from food and excluded the contribution from microbial activities. The two feeding scenarios resulted in a ~400-fold difference in the D-Ala-<sup>13</sup>C<sub>3</sub>, <sup>15</sup>N level in plasma, despite the total consumption of D-Ala-<sup>13</sup>C<sub>3</sub>, <sup>15</sup>N being less in the short-term experiment (~40 vs ~100 mg) (**Figure 3(a)**). Assuming similar D-Ala absorption efficiency through gut, this indicated that most of the orally administered D-Ala-<sup>13</sup>C<sub>3</sub>, <sup>15</sup>N were likely removed from the animal over time. We also determined that blood transported the gut-absorbed D-Ala-<sup>13</sup>C<sub>3</sub>, <sup>15</sup>N to tissues. In both feeding scenarios, we noticed that the ratio of D-Ala-<sup>13</sup>C<sub>3</sub>, <sup>15</sup>N over total unlabeled alanine in plasma was always among the highest in all samples (**Figure S1**) and positively correlated to the ratio in other samples (**Table S1**).

We obtained clear evidence of gut-absorbed D-Ala entering the central nervous system (CNS) and accumulating over time. Normalization of D-Ala-<sup>13</sup>C<sub>3</sub>, <sup>15</sup>N concentration (**Equation 1, 2, 3**) enabled comparisons between feeding scenarios and across sample types. Significantly higher levels of D-Ala-<sup>13</sup>C<sub>3</sub>, <sup>15</sup>N are found in the pituitaries (6-fold) and brains (42-fold) of the feeding group exposed to the isotope for 2-weeks compared to the exposed for 1-hour gavage group (**Figure 3b**). These findings suggest that D-Ala-<sup>13</sup>C<sub>3</sub>, <sup>15</sup>N accumulate in the pituitary and brain over time. The accumulation of D-Ala-<sup>13</sup>C<sub>3</sub>, <sup>15</sup>N in the brain with most blood removed also demonstrates that D-Ala can cross the blood-brain barrier. As D-Ala is a co-agonist of the NMDAR and found to have different concentrations in different parts of the brain, gut-absorbed D-Ala accumulation in the brain over time suggests a mechanism to regulate D-Ala levels, which may be related to its functions. For example, the correlation of D-Ala levels in rodents and humans with circadian rhythm has been reported (15–18), while the D-Ala concentration is reported to be high in the pineal gland (40). As both D-Ala and D-Ser interact with the same

NMDA receptor binding site, it will be interesting to determine how these two systems interact given one is endogenous and the other an exogenous molecule.

Previous evidence has pointed out the possibility of D-Ala being involved in regulation of glucose metabolism and the hypothalamus-pituitary-adrenal (HPA) axis, including immunostaining against D-Ala (19, 20) and detection of D-Ala change upon glucose stimulation (21). Interestingly, the circadian changes of D-Ala levels seem to also correlate to the feeding parameters and insulin levels (16) and differential gut absorption of D-Ala (17). We found that in both short- and long-term oral administration of D-Ala- $^{13}\text{C}_3$ ,  $^{15}\text{N}$ , the normalized D-Ala- $^{13}\text{C}_3$ ,  $^{15}\text{N}$  ratio in both the pancreatic islets and acinar tissues were always similar and among the highest measured (**Figure 3(c)(d)**), despite that the normalized D-Ala- $^{13}\text{C}_3$ ,  $^{15}\text{N}$  concentration in the pancreatic islets were much lower than that in acinar tissues (**Figure 3(b)**). The islets and acinar tissues in untreated animals also showed high levels of D-Ala% in both germ-free and regular mice (**Figure 2(a)**). Together, these findings indicate that the islets and acinar tissues can rapidly uptake gut-absorbed D-Ala and maintain a relatively stable level of D-Ala over time.

To provide additional insights on the possible impacts of gut-absorbed D-Ala on the function of the endocrine system including elements of the HPA axis, we performed MALDI-TOF MS measurements of the peptide profiles of pituitary and islets collected from animals administrated D-Ala- $^{13}\text{C}_3$ ,  $^{15}\text{N}$  or L-Ala-2,3,3,3- $\text{d}_4$  for 2-weeks (**Figure 4**). Due to the semi-quantitative nature of MALDI-TOF MS peptide profiling and the small sample size ( $n=4$ ), uncorrected multiple t-tests were used to maximize the number of molecular features differentiating the peptide profiles. Results showed that the two-week treatment of D-Ala or L-Ala isotopes resulted in differences in peptide profiles of both the pancreatic islets and pituitary glands. Several features were found specifically in data sets acquired from D-Ala-treated groups but not L-Ala-treated groups. Interestingly, in islets, normalized intensities of signals at  $m/z$  1952.0 (matching mouse insulin 1 fragment 61-79) and  $m/z$  5797.6 (matching to insulin) changed in opposite directions (**Figure 4(a)**). For the pituitary, treatment with L-Ala-2,3,3,3- $\text{d}_4$  resulted in more changes in peptide profiles compared to D-Ala- $^{13}\text{C}_3$ ,  $^{15}\text{N}$  treatment (**Figure 4(c)(d)**). Intensities of signal at  $m/z$  2586.4 (matches the phosphorylated form of CLIP, a fragment of ACTH), were found to decrease more than 2-fold upon D-Ala- $^{13}\text{C}_3$ ,  $^{15}\text{N}$  treatment, although the intensity of signal at  $m/z$  2506.4 (matches the non-phosphorylated CLIP) were not different. As no MS/MS structural characterization of detected features/peptides was done during the MALDI-TOF MS analysis, further investigation using LC-MS/MS is needed to confirm identities of some peptides such as insulin, ACTH, and related peptides and to quantify the changes of peptide levels related to the HPA axis upon D-Ala treatment.

## Conclusions

Using germ-free mice and stable isotopically labeled D-/L-Ala, we identified the sources and localization of D-Ala in the mouse, tracked gut-absorbed D-Ala biodistribution in various tissues, and explored the peptide/hormone profile changes in islets and pituitary gland after D-Ala administration. Our data demonstrated that D-Ala can be absorbed through both small intestines and colon, carried by blood into circulation, and distributed differentially in various tissues after both 1-hour and 2-week oral administration. Pancreatic islets and acinar tissues possessed the highest levels of gut-absorbed D-Ala. Interestingly, pituitary and brain tissues accumulated more of gut-absorbed D-Ala over the period of 2-week treatment compared to the 1-hour treatment via

one-time gavage, indicating the CNS and pituitary have specific mechanisms for the D-Ala uptake and storage. Observed pancreatic islet and pituitary peptide profile differences between control and 2-week treatment of D-Ala indicate the involvement of D-Ala in the HPA axis functions. Feeding germ-free and regular mice with stable isotope labeled L-Ala, we found that no alanine racemase activity was present in germ-free mice in contrast to experiments with bacterial culture and possessing microbiota regular mice. We conclude that microbiota and diet are two sources of D-Ala in mice, while no endogenous synthesis of D-Ala via racemization was reliably observed over the time period of our experimental design.

## Methods

**Materials and reagents.** D-Ala- $^{13}\text{C}_3$ ,  $^{15}\text{N}$  (Cat. #: 760277) and D-Ala-3,3,3- $\text{d}_3$  (Cat #: 642975) isotopes were obtained from Sigma Aldrich. L-Ala-3,3,3- $\text{d}_3$  (Cat #: DLM-248-1), and L-Ala-2,3,3,3- $\text{d}_4$  (Cat. #: DLM-250-PK), L-Leu-5,5,5- $\text{d}_3$  (Cat. #: DLM-1259), and L-Ser- $^{13}\text{C}$ ,  $^{15}\text{N}$  (Cat. #: CNLM-7814) isotopes were obtained from Cambridge Isotope Laboratories. Unlabeled L-Ala was purchased from Fluka and D-Ala was from Sigma Aldrich. A set of 20G 1.5" reusable stainless feeding needle (N-PK) was purchased from Braintree Scientific, Inc. Methanol (Cat. #: A456) and  $\text{H}_2\text{O}$  (Cat. #: W64), Optima™ LC/MS Grade, were purchased from Fisher Scientific.

**Animals.** Animal experiments were performed following the animal use protocol #19251 approved by the Institutional Animal Care and Use Committee (IACUC) at the University of Illinois Urbana-Champaign (UIUC). Germ-free C57BL/6 male mice (9-11 weeks old) were obtained from the Rodent Gnotobiotic Facility at the UIUC. Regular C57BL/6 inbred male mice (8 weeks old) were purchased from Envigo and housed in the animal facility at the Beckman Institute (UIUC). All mice were housed as 2 animals per cage. Both germ-free and regular mice were fed with sterilized 2019S Teklad Global 19% Protein Extruded Rodent Diet (Sterilizable) from Envigo.

### Stable isotope feeding.

**Gavage.** Solutions of 0.9% NaCl and 150 mg/mL D-Ala- $^{13}\text{C}_3$ ,  $^{15}\text{N}$  were made and filtered with 0.22  $\mu\text{m}$  PVDF sterile filter. With proper sterile procedures, sealed positive pressure individual ventilated cages holding 10-week-old germ-free C57BL/6 mice, as well as solutions and tools, were transferred to a biosafety cabinet (BSC). All materials were autoclaved/sterile filtered previously and sanitized immediately before sending into the BSC through specifically design portal. Each germ-free mouse was weighed inside of the BSC and orally administrated with 260-270  $\mu\text{L}$  (10 mL/kg body mass) of saline or D-Ala- $^{13}\text{C}_3$ ,  $^{15}\text{N}$  solution (1.5 g/kg body mass) in the BSC, transferred back to its original cage, and sent back to the rack. To minimize the impact of circadian rhythm on alanine levels in mice, gavage experiments were performed around the same time each day (~11 am). After 60 minutes, the mice were sent for euthanasia and dissection. Each gavage experiment included 4 mice (2 for saline and 2 for D-Ala- $^{13}\text{C}_3$ ,  $^{15}\text{N}$ ). The experiment was repeated twice. For regular animals treated with L-Ala-2,3,3,3- $\text{d}_4$ , animals were fed with the same food as germ-free mice for 2 weeks after they arrive at our facility before experiments, and solutions of 0.9% NaCl and 150 mg/mL of L-Ala-2,3,3,3- $\text{d}_4$  were orally administrated with 10 mL/kg body mass of saline or L-Ala-2,3,3,3- $\text{d}_4$  (1.5 g/kg body mass). The gavage experiment included 6 mice (3 for saline and 3 for L-Ala-2,3,3,3- $\text{d}_4$ ) following the same timeline as the germ-free experiments.

**Feeding.** Solutions of 1.25 g/L D-Ala-<sup>13</sup>C<sub>3</sub>,<sup>15</sup>N and L-Ala-2,3,3,3-d<sub>4</sub> were made using the same tap water used to feed germ-free mice, autoclaved, sent into the BSC with proper sterile procedures, and used to fill water bottles installed in mice cages. Inside of the BSC, water bottles containing sterile tap water, tap water supplemented with D-Ala-<sup>13</sup>C<sub>3</sub>,<sup>15</sup>N, or tap water supplemented with L-Ala-2,3,3,3-d<sub>4</sub> were installed into cages already containing 9-10 weeks old mice and the cages were returned to the rack. During the two-week treatment, water levels in the mice cage were monitored by eyes every other day and refilled when necessary. Each feeding experiment included 6 mice (2 for each condition) and the experiment was repeated twice.

**Dissection and sample collection.** After treatment time ended, animals were transported to a clean procedure room or a necropsy suite around noon, euthanized by CO<sub>2</sub> asphyxiation, and followed by tissue collection occurring during afternoon hours. Blood was drawn using a disposable 1 mL syringe directly from the heart after being cut open, transferred into a BD Microtainer tube (Cat. # 365965) and settled on ice. Plasma was separated by centrifugation of a BD Microtainer tube (lithium heparin) at 3000 x g for 10 minutes at room temperature. Animals were then perfused with cold modified Gey's balanced salt solution (mGBSS) containing (in mM) 1.5 CaCl<sub>2</sub>, 4.9 KCl, 0.2 KH<sub>2</sub>PO<sub>4</sub>, 11 MgCl<sub>2</sub>, 0.3 MgSO<sub>4</sub>, 138 NaCl, 27.7 NaHCO<sub>3</sub>, 0.8 Na<sub>2</sub>HPO<sub>4</sub>, 25 HEPES, pH 7.2. mGBSS buffer through the heart. Mouse pancreata were perfused with a small volume of cold digestive solution (see below for details) and collected for the isolation of islets and acinar tissues. Gastrointestinal tracts, including the small intestine and colon, were cut open longitudinally to collect small intestine and colon contents, and the GI tract tissues were rinsed several times in ice-cold PBS buffer before collection. Brain, salivary glands, and pituitary glands were collected as well. All tissues and gut contents, as well as separated plasma, were set on dry ice immediately after collection and stored at -80C until the next steps.

**Isolation of islet of Langerhans from mouse pancreas.** 1.06 Wunsch unit of Liberase TL (Sigma) and 0.1 mg/mL of DNase I recombinant (deoxyribonuclease) prepared in Hank's balanced buffer solution (HBSS, GIBCO) with 5 mM calcium chloride and 25 mM HEPES (Sigma) and sit on ice until use. A 2 mL of this enzymatic solution was perfused into the mouse pancreas through the common bile duct. The perfused pancreata were removed from the body and placed in conical tubes with 5 mL of cold Liberase solution on the ice. The tubes were placed in the pre-warmed water bath at 37°C for 10 min for digestion. At the end of incubation, cold HBSS with 0.2% bovine serum albumin were added into tubes and the tubes were shaken vigorously to ensure the islets were completely separated from the tissue. After the centrifugation at 300 g for 3 min, the supernatant was removed. These steps were repeated 3 times. At the last step, the supernatant was poured out by decanting and leftover buffer inside the tube were mechanically removed. Subsequently, pellets of digested tissue were resuspended in 7 mL sterile Histopaque 1077 solution (Sigma) with gentle shaking. 3 mL of cold HBSS buffer was layered on the top of the tissue suspension and the tubes were centrifuged at 900 g for 15 min. The islets located in the supernatants were filtered through 70 µm sterile cell strainer and washed 3 times using Cold HBSS to remove cell debris. The purified islets were placed into a Petri dish filled with cold HBSS, quickly manually picked and transferred to the cold acidified MeOH for analyte extraction (MeOH:H<sub>2</sub>O:acetic acid 90:9:1 by volume).

**Bacteria exposure to isotope and biomass collection.** *Escherichia coli* (*E. coli*) strain OP50 were grown on a Luria-Bertani (LB) agar plates, and single colonies were picked and inoculated into a bottle of 100 mL liquid LB broth for overnight growth. On the next day, aliquots of 5 mL of

overnight *E. coli* liquid culture were transferred to sterile culture tubes, and 1 mL of 1.25 g/L sterile L-Ala-2,3,3,3-d<sub>4</sub> solution or autoclaved water were added. Aliquots of 1 mL bacterial liquid culture were collected before adding isotope and 1- and 5-hours after adding isotope. Biomass was collected by centrifugation at 16,000 x g for 1 minute, supernatant removed with a 1-mL pipet tip, centrifuged again, the remaining supernatant removed with a 200- $\mu$ L pipet tip, centrifuged, and formed supernatant removed using a 10- $\mu$ L pipet tip. Resulting pelleted biomass was weighed and frozen at -80 °C until amino acid extraction.

### **Sample processing and analyte extraction.**

*Brain/salivary gland/small intestine/colon/mouse chow samples.* Frozen samples of the brain, salivary gland, small intestine, colon, or mouse chow were crushed using either a metal tissue pulverizer or a metal hammer on a flat metal surface, and all metal parts were kept cold on dry ice throughout. Crushed cold flakes of samples were then quickly transferred to a 2 mL tissue homogenizing CKMix tube. After weighing, 600  $\mu$ L of ice-cold 1:1 MeOH:H<sub>2</sub>O was added for tissue homogenization using a Precellys® Evolution tissue homogenizer with a cold trap (Bertin Corp.). Samples were homogenized at 2x30s with one 30s pause at 7200 rpm twice, and the resulting suspensions were transferred and centrifuged at 12,000 x g for 20 minutes at 4 °C. The supernatant was transferred to another tube and dried using a Genevac™ miVac Centrifugal Concentrator. The remaining pellet was added with 600  $\mu$ L of ice-cold water, followed by vortex, sonication, and centrifugation at 12,000 x g for 20 minutes at 4 °C. The aqueous supernatant was collected, added to the dried tube previously used for methanol supernatant collection, and dried using the vacuum concentrator. Resulting samples were stored in -20 °C until the next steps.

*Small intestine content and colon content samples.* Frozen samples were thawed, and disposable spatulas were used to scoop and transfer part of sample to a tissue homogenizing CKMix tube. The same sample processing and analyte extraction steps as for brain/salivary gland/intestine samples were followed.

*Plasma samples.* Frozen plasma samples were thawed and 40  $\mu$ L of plasma was transferred to a new tube. 600  $\mu$ L of 1:1 MeOH:H<sub>2</sub>O and 600  $\mu$ L of H<sub>2</sub>O were sequentially added to extract from plasma samples. The resulting supernatants were combined, dried, and stored using the same procedure above.

*Pituitary samples.* A procedure including boiling water, acidified MeOH and 0.25% acetic acid solution was used to extract amino acids and peptides from pituitary gland samples. To the frozen pituitary samples, 400  $\mu$ L of pre-heated 90 °C water was added, followed by a 10-min incubation in a boiling water bath. Samples were immediately cooled down on ice. A hand homogenizer with disposable plastic pestle was used to disrupt and homogenize samples, followed by centrifugation at 12,000 x g for 15 minutes at 4 °C. Supernatants were collected, transferred to Low Protein Binding Collection Tubes (Thermo Fisher), and evaporated to dryness using the Genevac concentrator. The same extraction procedure was repeated with 400  $\mu$ L of acidified MeOH and 400  $\mu$ L of 0.25% acetic acid, except bath sonication was used instead of hand homogenizer. Dried samples were stored in -20 °C until further use.

*Islets/acinar tissue samples.* Islets and acinar tissues stored in 400  $\mu$ L of acidified MeOH were homogenized with a hand homogenizer based on disposable plastic pestle, followed by centrifugation at 15,000 x g for 15 minutes at 4 °C. Supernatants were transferred to a new low

protein binding tube. The remaining pellets were extracted by 400  $\mu$ L of MeOH and 400  $\mu$ L of water using bath sonication. All three supernatants were combined, mixed, aliquoted, and evaporated to dryness. Dried samples were stored at -20 °C until further use.

*Cleanup of sample extracts.* Extracts of brain, salivary glands, intestines, gut contents, plasma, and mouse chow samples were further processed using centrifugal filters. Dried extracts were reconstituted in 300  $\mu$ L of 33-100  $\mu$ M L-Leu-5,5,5- $d_3$  solution in water, followed by vortexing, sonication, and centrifugation at 16,000 x g for 15 minutes at 4 °C. Supernatants were then filtered with a 0.45  $\mu$ m Nanosep MF centrifugal devices with Bio-Inert® membrane at 10,000 x g for 15 minutes at 4 °C followed by filtration by a 3K Nanosep® centrifugal devices with Omega™ membrane at 10,000 x g for 65-75 minutes at 4 °C. Filtrates were then dried using an Eppendorf Vacufuge concentrator and stored at -20 °C until the next steps.

*Extraction of analytes from bacterial biomass.* Frozen bacterial biomass was thawed and 300  $\mu$ L MeOH was added to each sample. Biomass was dispersed in MeOH by repetitive pipetting, followed by bath sonication for 10 minutes or until visibly fully dispersed. The resulting suspension was centrifuged at 16,000 x g for 2 minutes and the supernatant was collected. The remaining pellets were further extracted with 300  $\mu$ L water, and the supernatant was collected. Supernatants from two rounds of analyte extraction for the same sample were combined and dried using an Eppendorf Vacufuge concentrator and stored at -20 °C until the next steps.

**MALDI-TOF mass spectrometry peptide profiling and data analysis.** Pituitary, islets, and acinar tissue samples were reconstituted in 40  $\mu$ L of 0.1% trifluoroacetic acid solution in water. Reconstituted samples were centrifuged at 12-14,000 x g for 15 minutes at 4 °C. 0.5  $\mu$ L of supernatants was mixed with equal volumes of alpha-cyano-4-hydroxycinnamic acid (CHCA) solution on sample plate and dried. MALDI-TOF MS analysis was performed using a ultrafleXtreme II system (Bruker Daltonics, Billerica, MA) operating in positive mode. Range of m/z 800-6000 was examined in reflector mode. After taking aliquots for BCA assay, the rest of the extracts were dried and stored at -20 °C. Mass spectra were analyzed using the flexAnalysis software (Bruker). Peaks were automatically or manually picked, peak lists created and compared to published information on mouse islets and pituitary peptides (30–34). Only peaks that appeared in at least 10 out of total 12 samples were added to final mass lists (see **Supporting Information**). Peak intensities were then normalized to the total intensity of selected m/zs observed in the same sample, followed by log<sub>2</sub> transformation. Uncorrected multiple t-tests were used to determine the differences of log<sub>2</sub>-transformed normalized peak intensities between the control and treated groups and results were presented in form of volcano plots.

**BCA total protein content assay.** BCA total protein content assay was performed on the pituitary, islets, and acinar tissue samples using either Pierce™ BCA Protein Assay (Thermo Fisher, Cat. #: 23225) or Micro BCA™ Protein Assay (Thermo Fisher, Cat. #: 23235). A sample volume of 1-2  $\mu$ L was taken from reconstituted samples prepared for MALDI-TOF MS analysis and diluted according to the manufacturer's protocol. Calibration curves of 0-40  $\mu$ g/mL were built for assays.

**Chiral amino acid analysis.**

*Marfey's reaction.* A variation of Marfey's reagent,  $N_{\alpha}$ -(2,4-dinitro-5-fluorophenyl)-L-valinamide (FDVA, Cat. # 42102, Sigma), was used to react with free amines of analytes present in samples to aid the separation of L/D-Ala using reverse-phase liquid chromatography and analyte quantification using mass spectrometry (42). Dried samples were reconstituted in 100 or 120  $\mu$ L 0.5M  $\text{NaHCO}_3$  solution (50  $\mu$ L for pituitary samples, 22  $\mu$ L for islets/acinar samples). Standards series of L/D-Ala (4-800  $\mu$ M for L and 0.1-40  $\mu$ M for D), D-Ala- $^{13}\text{C}_3,^{15}\text{N}$  (10  $\mu$ M-4 mM), L/D-Ala-3,3,3- $\text{d}_3$  (2-400  $\mu$ M for L and 1-200  $\mu$ M for D), and L-Ala-2,3,3,3- $\text{d}_4$  (1-400  $\mu$ M), and L-serine- $^{13}\text{C},^{15}\text{N}$  (4 mM, as internal standard at LC injection) were made in 0.5M  $\text{NaHCO}_3$  as well. FDVA was weighed using an analytical balance and dissolved in acetonitrile to a final concentration of 5-6 mg/mL (1 mg/mL for islets/acinar samples). Reconstituted samples were centrifuged at 16,000 g for 5 minutes at 4°C, and 10  $\mu$ L aliquots of supernatants or supernatants diluted into 0.5M  $\text{NaHCO}_3$  were mixed with 10  $\mu$ L of FDVA solution in 0.2 mL PCR tubes (except for 20  $\mu$ L samples and 20  $\mu$ L FDVA solution for islets and acinar tissue samples). Standards were directly mixed 1:1 with FDVA solution at the same volumes. The mixtures were reacted at 60°C for 3 hours in a Bio-Rad T100 thermal cycler. After the reaction, mixtures were either immediately subject to analysis or frozen at -80°C until analysis.

*Desalting and concentrating Marfey's reaction for islets/acinar tissue samples.* Due to the low levels of amino acids extracted from islets and acinar tissue samples, Pierce™ Peptide Desalting Spin Columns (Thermo Fisher, Cat. #: 89851) were used to desalt and concentrate derivatized amino acids from reacted islets and acinar tissue samples. Finished Marfey's reactions were dried using the Eppendorf Vacufuge concentrator and reconstituted in 150  $\mu$ L of 0.1% TFA in water, followed by steps in the manufacturer's protocol with several minor modifications to maximize the recovery. Eluted solutions were then dried and stored in -20 °C until analysis.

*LC-MS/MS analysis.* An LC-MS/MS analysis was performed in multiple reaction monitoring (MRM) mode. MRM allows quantitation of the L/D-amino acid contents of the samples. Elute ultra-high performance liquid chromatography (UHPLC) coupled to a Bruker EVOQ triple quadrupole mass spectrometer operating in negative ESI mode was used in MRM measurements (42). The MRM channels were built using amino acid standards reacted with FDVA; details of source parameters and MRM transitions can be found in **Table S3 and S4**. Derivatized L/D-amino acids were separated using a Kinetex® 2.6  $\mu$ m Phenyl-Hexyl 100 Å, 100 x 2.1 mm column (Phenomenex, Cat. #: 00D-4495-AN) at 30 °C. A gradient of 25 mM ammonium formate in water (A) and methanol (B) was used at a flow rate of 0.3 mL/min. The gradient is 0-2min, 95% A; 2-3.5min, 95%-78% A; 3.5-6min, 78%-50% A; 6-9min, 50%-45% A; 9-9.5min, 45%-10% A; 9.5-11min, 10% A; 11-11.5min, 10%-95%A; 11.5-12min, 95% A.

To perform LC-MS/MS analysis, the reaction mixtures were centrifuged at 16,000 g for 5 minutes at 4°C and then diluted 20 to 80-folds (mostly 40-folds) into the loading buffer consisting of 95% mobile phase A, 5% acetonitrile and 2  $\mu$ M of FDVA-L-Ser- $^{13}\text{C},^{15}\text{N}$  as an internal control. Standards were diluted at least 40-folds by the loading buffer. At least two technical sample injections were done for all samples within each LC-MS run. For long continuous LC-MS runs, calibration curves were run at the beginning, in the middle, and at the

end of the whole sample list, and a master calibration curve was summarized by averaging all calibration curves. FDVA peak areas were monitored for all samples to calculate the leftover amount of FDVA remaining after Marfey's reactions and compared to reaction blanks. If the FDVA content in the samples (leftover FDVA) was less than 20% of the reaction blank, the reconstituted samples were further diluted and re-reacted until the leftover FDVA was more than 20%. All samples were measured at least twice on different days by two independent operators.

### **LC-MS/MS data analysis and statistics**

*LC-MS/MS data analysis.* Peak areas integrated by MS Data Viewer software (Bruker) were used for quantification. Calibration curves covered ranges from 0.2-120 pmole for L-Ala, 0.005-3 pmole for D-Ala, 0.2-200 pmole for D-Ala-<sup>13</sup>C<sub>3</sub>, <sup>15</sup>N, 0.005-2 for L-Ala-3,3,3-d<sub>3</sub>, 0.0025-1 pmole for D-Ala-3,3,3-d<sub>3</sub>, 0.0025-1 pmole for L-Ala-2,3,3,3-d<sub>4</sub>, and 0.1-30 pmole for L-Leu-5,5,5-d<sub>3</sub> per injection. Peak areas were normalized to the peak area of L-Ser-<sup>13</sup>C, <sup>15</sup>N present in the same sample by division. Linear regressions were fit at proper ranges that best covers the detected peak areas in the unknown samples. When necessary, linear regressions were done in two segments for the same analyte to best cover the high and low concentration ranges; for low concentration range calibration curves, the calibration curve were set to intercept at (0,0). All linear regressions achieved R square >0.99 with very several exceptions. After quantification of AAs per injection in unknown samples using peak areas and calibration curves, amounts of not labeled Ala, isotopically labeled Ala, and L-Leu-5,5,5-d<sub>3</sub> were calculated for reconstituted samples and blanks. Results of technical replicates were averaged. Analyte recovery after centrifugal filtration step were represented via dividing the amount of L-Leu-5,5,5-d<sub>3</sub> in unknown samples by the amounts of L-Leu-5,5,5-d<sub>3</sub> in reference samples, and was used to calculate back the concentration of Ala in original sample extraction before filtration. Blank values were then subtracted from values of corresponding analyte signal detected in each set of samples, and the levels of not labeled and stable isotope labeled Ala were calculated by dividing by different sample metrics (e.g., tissue weight in mg for brain/salivary glands/intestines/pituitary/mouse chow, gut contents weights in mg,  $\mu$ L for plasma, total protein amounts for islets/acinar tissues). The individual processed values can be found in **Supporting Information**.

*Statistics.* Non-parametric statistics were implemented for all data obtained from LC-MS measurements. Initially, Welch's t-tests were performed due to unequal sample sizes and unequal variances. However, due to the small degree of freedom in parametric Welch's t-tests, non-parametric Mann-Whitney tests were chosen for individual pairwise comparisons. For datasets in **Figure 2**, **Figure 3(b)**, **Figure 5(b)(c)(d)(e)**, two-tailed Mann-Whitney tests were used. For datasets in **Figure 5(f)(g)(h)(i)(j)**, one-tailed Mann-Whitney tests were used because of the sample size (n=3) and the complete separation observed in the dataset. Non-parametric Kruskal-Wallis one-way ANOVA followed by Dunn's multiple comparison were used to determine if tissue types significantly contribute to D-Ala-<sup>13</sup>C<sub>3</sub>, <sup>15</sup>N level and investigate the differences among tissue types (**Figure 4(c)(d)**). Significance level ( $\alpha$ ) for all statistics is set to 0.05 when describing statistical significance. All statistics were done in GraphPad Prism 9.2.0.

### **Data availability**

The processed data supporting the conclusions are presented in the main text and Supporting Information. The original data are available and will be shared upon request by contacting the corresponding author or the lead author ([qiutian8@msu.edu](mailto:qiutian8@msu.edu)).

*Supporting information*—This article contains supporting information.

*Acknowledgements*—We thank Dr. Fuming Pan and J. Reid McClure at the UIUC Rodent Gnotobiotic Facility for their assistance in germ-free animal experiments. We thank Nissa J. Larson for her help in the BCA experiments and Elena V. Romanova and Peter Chan-Andersen for their help in mass spectrometry experiments on peptide profiling. We thank Theren Williams at the Illinois Statistics Office for his help in statistics.

*Author contributions*—**Tian (Autumn) Qiu**: Conceptualization, Methodology, Validation, Formal analysis, Investigation, Visualization, Writing – Original Draft, Writing – Review & Editing, Project administration, Funding acquisition, **Cindy J. Lee**: Methodology, Validation, Formal analysis, Investigation, Writing – Review & Editing, **Chen Huang**: Formal analysis, Investigation, Writing – Original Draft, **Stanislav S. Rubakhin**: Methodology, Validation, Resources, Writing – Review & Editing, **Dongkyu Lee**: Methodology, Resources, Writing – Original Draft, **Jonathan V. Sweedler**: Conceptualization, Resources, Writing – Review & Editing, Supervision, Funding acquisition

*Funding*—This work was supported by a Beckman Institute Postdoctoral Fellowship at UIUC from the Arnold and Mabel Beckman Foundation and a Mistletoe Research Fellowship from the Momental Foundation (T.A.Q.), by the Pilot Project Grant Program from Office of the Vice Chancellor for Research at University of Illinois, by Award No. R01NS031609 from the National Institute of Neurological Disorders and Stroke of the National Institutes of Health (J.V.S.), and by support from the American Diabetes Association Pathway to Stop Diabetes Grant No. 1-18-VSN-19 (J.V.S.). The content is solely the responsibility of the authors and does not necessarily represent the official views of the funding agencies.

*Conflict of interest*—The authors declare that they have no known competing financial interests or personal relationships that could have appeared to influence the work reported in this paper.

*Abbreviations*— The abbreviations used are: AA, amino acid; ACN, acetonitrile; ACTH, adrenocorticotropin; D-AA, D-amino acid; D-Ala, D-alanine; ANOVA, analysis of variance; CLIP, corticotropin-like intermediate peptide; CNS, central nervous systems; FDVA, N<sub>α</sub>-(2,4-dinitro-5-fluorophenyl)-L-valinamide; HPA, hypothalamus-pituitary-adrenal; L-AA, L-amino acid; L-Ala, L-alanine; LPH, lipotropin; LB, Luria-Bertani; MALDI-TOF, matrix-assisted laser desorption/ionization time-of-flight; MRM, multiple reaction monitoring; NMDAR, N-methyl-D-aspartate receptor;

## References:

1. Adams, J. B., Johansen, L. J., Powell, L. D., Quig, D., and Rubin, R. A. (2011) Gastrointestinal flora and gastrointestinal status in children with autism – comparisons to typical children and correlation with autism severity. *BMC Gastroenterol.* **11**, 22
2. Wu, S., Liu, X., Jiang, R., Yan, X., and Ling, Z. (2021) Roles and mechanisms of gut microbiota in patients with Alzheimer's disease. *Front Aging Neurosci.* **13**, 650047
3. Klann, E. M., Dissanayake, U., Gurralla, A., Farrer, M., Shukla, A. W., Ramirez-Zamora, A., Mai, V., and Vedam-Mai, V. (2022) The gut–brain axis and its relation to Parkinson's disease: a review. *Front Aging Neurosci.* **13**, 782082
4. Wang, Z., and Zhao, Y. (2018) Gut microbiota derived metabolites in cardiovascular health and disease. *Protein Cell.* **9**, 416–431
5. Di Meo, F., Margarucci, S., Galderisi, U., Crispi, S., and Peluso, G. (2019) Curcumin, gut microbiota, and neuroprotection. *Nutrients.* **11**, 2426
6. Sanna, S., van Zuydam, N. R., Mahajan, A., Kurilshikov, A., Vich Vila, A., Vösa, U., Mujagic, Z., Masclee, A. A. M., Jonkers, D. M. A. E., Oosting, M., Joosten, L. A. B., Netea, M. G., Franke, L., Zhernakova, A., Fu, J., Wijmenga, C., and McCarthy, M. I. (2019) Causal relationships among the gut microbiome, short-chain fatty acids and metabolic diseases. *Nat Genet.* **51**, 600–605
7. Pokusaeva, K., Johnson, C., Luk, B., Uribe, G., Fu, Y., Oezguen, N., Matsunami, R. K., Lugo, M., Major, A., Mori-Akiyama, Y., Hollister, E. B., Dann, S. M., Shi, X. Z., Engler, D. A., Savidge, T., and Versalovic, J. (2017) GABA-producing *Bifidobacterium dentium* modulates visceral sensitivity in the intestine. *Neurogastroenterol Motil.* **29**, e12904
8. Cava, F., Lam, H., de Pedro, M. A., and Waldor, M. K. (2011) Emerging knowledge of regulatory roles of D-amino acids in bacteria. *Cell Mol Life Sci.* **68**, 817–831
9. Mothet, J.-P., Le Bail, M., and Billard, J.-M. (2015) Time and space profiling of NMDA receptor co-agonist functions. *J Neurochem.* **135**, 210–225
10. Mothet, J.-P., Parent, A. T., Wolosker, H., Brady, R. O., Linden, D. J., Ferris, C. D., Rogawski, M. A., and Snyder, S. H. (2000) D-Serine is an endogenous ligand for the glycine site of the N-methyl-D-aspartate receptor. *Proc Natl Acad Sci.* **97**, 4926–4931
11. Wolosker, H. (2007) NMDA receptor regulation by D-serine: new findings and perspectives. *Mol Neurobiol.* **36**, 152–164
12. MacKay, M.-A. B., Kravtzenyuk, M., Thomas, R., Mitchell, N. D., Dursun, S. M., and Baker, G. B. (2019) D-Serine: potential therapeutic agent and/or biomarker in schizophrenia and depression? *Front Psychiatry.* **10**, 25
13. Kleckner, N. W., and Dingledine, R. (1988) Requirement for glycine in activation of NMDA-receptors expressed in *Xenopus* oocytes. *Science.* **241**, 835–837
14. McBain, C. J., Kleckner, N. W., Wyrick, S., and Dingledine, R. (1989) Structural requirements for activation of the glycine coagonist site of N-methyl-D-aspartate receptors expressed in *Xenopus* Oocytes. *Mol Pharmacol.* **36**, 556–565
15. Morikawa, A., Hamase, K., and Zaitzu, K. (2003) Determination of D-alanine in the rat central nervous system and periphery using column-switching high-performance liquid chromatography. *Anal Biochem.* **312**, 66–72

16. Morikawa, A., Hamase, K., Miyoshi, Y., Koyanagi, S., Ohdo, S., and Zaitso, K. (2008) Circadian changes of D-alanine and related compounds in rats and the effect of restricted feeding on their amounts. *J Chromatogr. B.* **875**, 168–173
17. Karakawa, S., Miyoshi, Y., Konno, R., Koyanagi, S., Mita, M., Ohdo, S., and Hamase, K. (2013) Two-dimensional high-performance liquid chromatographic determination of day–night variation of D-alanine in mammals and factors controlling the circadian changes. *Anal. Bioanal Chem.* **405**, 8083–8091
18. Morikawa, A., Fukuoka, H., Uezono, K., Mita, M., Koyanagi, S., Ohdo, S., Zaitso, K., and Hamase, K. (2017) Sleep-awake profile related circadian D-alanine rhythm in human serum and urine. *Chromatography.* **38**, 53–58
19. Morikawa, A., Hamase, K., Ohgusu, T., Etoh, S., Tanaka, H., Koshiishi, I., Shoyama, Y., and Zaitso, K. (2007) Immunohistochemical localization of D-alanine to  $\beta$ -cells in rat pancreas. *Biochem. Biophys Res Commun.* **355**, 872–876
20. Etoh, S., Hamase, K., Morikawa, A., Ohgusu, T., and Zaitso, K. (2009) Enantioselective visualization of D-alanine in rat anterior pituitary gland: localization to ACTH-secreting cells. *Anal Bioanal Chem.* **393**, 217–223
21. Ota, N., Rubakhin, S. S., and Sweedler, J. V. (2014) D-Alanine in the islets of Langerhans of rat pancreas. *Biochem Biophys Res Commun.* **447**, 328–333
22. Lee, C. J., Schnieders, J. H., Rubakhin, S. S., Patel, A. V., Liu, C., Naji, A., and Sweedler, J. V. (2022) D-Amino acids and classical neurotransmitters in healthy and Type 2 diabetes-affected human pancreatic islets of Langerhans. *Metabolites.* **12**, 799
23. Lee, C. J., Qiu, T. A., and Sweedler, J. V. (2020) D-Alanine: distribution, origin, physiological relevance, and implications in disease. *Biochim Biophys Acta BBA - Proteins Proteomics.* **1868**, 140482
24. Marcone, G. L., Rosini, E., Crespi, E., and Pollegioni, L. (2020) D-Amino acids in foods. *Appl Microbiol Biotechnol.* **104**, 555–574
25. Lee, C. J., Qiu, T. A., Hong, Z., Zhang, Z., Min, Y., Zhang, L., Dai, L., Zhao, H., Si, T., and Sweedler, J. V. (2022) Profiling of D-alanine production by the microbial isolates of rat gut microbiota. *FASEB J.* **36**, e22446
26. Wei, Y., Qiu, W., Zhou, X.-D., Zheng, X., Zhang, K.-K., Wang, S.-D., Li, Y.-Q., Cheng, L., Li, J.-Y., Xu, X., and Li, M.-Y. (2016) Alanine racemase is essential for the growth and interspecies competitiveness of *Streptococcus mutans*. *Int J Oral Sci.* **8**, 231–238
27. Hols, P., Defrenne, C., Ferain, T., Derzelle, S., Delplace, B., and Delcour, J. (1997) The alanine racemase gene is essential for growth of *Lactobacillus plantarum*. *J Bacteriol.* **179**, 3804–3807
28. Mochizuki, T., Takayama, T., Todoroki, K., Inoue, K., Min, J. Z., and Toyo'oka, T. (2015) Towards the chiral metabolomics: liquid chromatography–mass spectrometry based DL-amino acid analysis after labeling with a new chiral reagent, (S)-2,5-dioxopyrrolidin-1-yl-1-(4,6-dimethoxy-1,3,5-triazin-2-yl)pyrrolidine-2-carboxylate, and the application to saliva of healthy volunteers. *Anal Chim Acta.* **875**, 73–82
29. Yoshikawa, M. (2022) Free D-amino acid in salivary gland in rat. *Biology* **11**(3), 390
30. Boonen, K., Baggerman, G., Hertog, W. D., Husson, S. J., Overbergh, L., Mathieu, C., and Schoofs, L. (2007) Neuropeptides of the islets of Langerhans: a peptidomics study. *Gen Comp Endocrinol.* **152**, 231–241

31. Toriumi, C., and Imai, K. (2002) Determination of insulin in a single islet of langerhans by high-performance liquid chromatography with fluorescence detection. *Anal Chem.* **74**, 2321–2327
32. Che, F.-Y., and Fricker, L. D. (2005) Quantitative peptidomics of mouse pituitary: comparison of different stable isotopic tags. *J Mass Spectrom.* **40**, 238–249
33. Che, F.-Y., Lim, J., Pan, H., Biswas, R., and Fricker, L. D. (2005) Quantitative neuropeptidomics of microwave-irradiated mouse brain and pituitary. *Mol Cell Proteomics.* **4**, 1391–1405
34. Romanova, E. V., Rubakhin, S. S., and Sweedler, J. V. (2008) One-step sampling, extraction, and storage protocol for peptidomics using dihydroxybenzoic acid. *Anal. Chem.* **80**, 3379–3386
35. Csapò, J., Albert, Cs., and Csapò-Kiss, Zs. (2009) The D-amino acid content of foodstuffs (a review). *Acta Univ Sapientiae Aliment.* **2**, 5–30
36. Brückner, H., and Schieber, A. (2001) Ascertainment of D-amino acids in germ-free, gnotobiotic and normal laboratory rats. *Biomed Chromatogr.* **15**, 257–262
37. Nagata, Y., Higashi, M., Ishii, Y., Sano, H., Tanigawa, M., Nagata, K., Noguchi, K., and Urade, M. (2006) The presence of high concentrations of free D-amino acids in human saliva. *Life Sci.* **78**, 1677–1681
38. Nagata, Y., Yamada, R., Nagasaki, H., Konno, R., and Yasumura, Y. (1991) Administration of D-alanine did not cause increase of D-amino acid oxidase activity in mice. *Experientia.* **47**, 835–838
39. Nagata, Y., Konno, R., and Niwa, A. (1994) Amino acid levels in D-alanine-administered mutant mice lacking D-amino acid oxidase. *Metabolism.* **43**, 1153–1157
40. Morikawa, A., Hamase, K., Inoue, T., Konno, R., and Zaitso, K. (2007) Alterations in D-amino acid levels in the brains of mice and rats after the administration of D-amino acids. *Amino Acids.* **32**, 13–20
41. Horio, M., Fujita, Y., Ishima, T., Iyo, M., Ferraris, D., Tsukamoto, T., and Hashimoto, K. (2009) Effects of D-amino acid oxidase inhibitor on the extracellular D-alanine levels and the efficacy of D-alanine on dizocilpine-induced prepulse inhibition deficits in mice. *Open Clin Chem. J.* **2**, 16–21
42. Livnat, I., Tai, H.-C., Jansson, E. T., Bai, L., Romanova, E. V., Chen, T., Yu, K., Chen, S., Zhang, Y., Wang, Z., Liu, D., Weiss, K. R., Jing, J., and Sweedler, J. V. (2016) A D-amino acid-containing neuropeptide discovery funnel. *Anal Chem.* **88**, 11868–11876

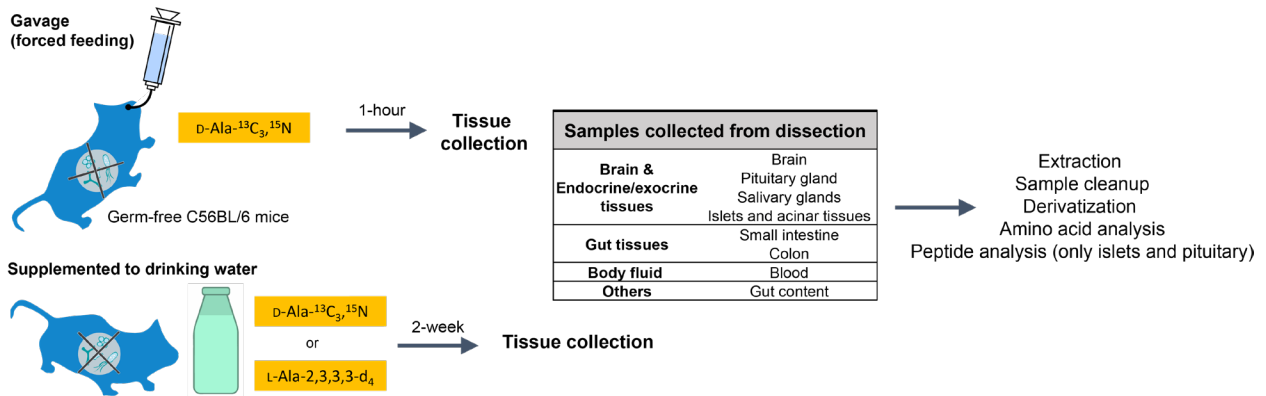


**Figure 1.** The experimental scheme for determination of L/D-alanine biodistribution and racemization.

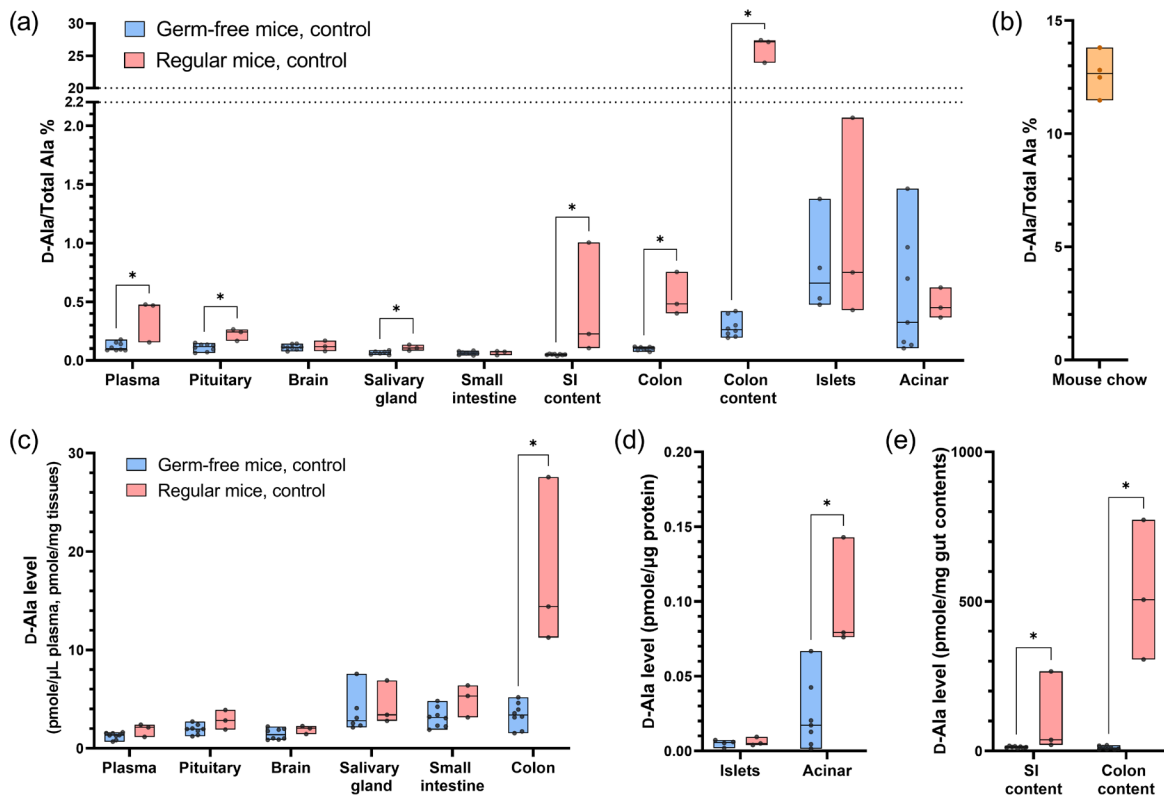


**Figure 2.** Endogenous, unlabeled D-Ala percentages (D-Ala/(L-Ala+D-Ala)%) (a) and concentrations (c)(d)(e) in samples from germ-free and regular mice, as well as the percentages in mice chow (b). Asterisks indicate the pairwise comparisons with statistical significance ( $\alpha=0.05$ ) from Mann-Whitney tests. Each data point represents one sample from one individual animal; for mouse chow, four data points represents four samples taken from two batches of food (1 and 3 samples for each batch). Floating bars indicate minimum and maximum, and the middle lines indicate median. SI – small intestine.

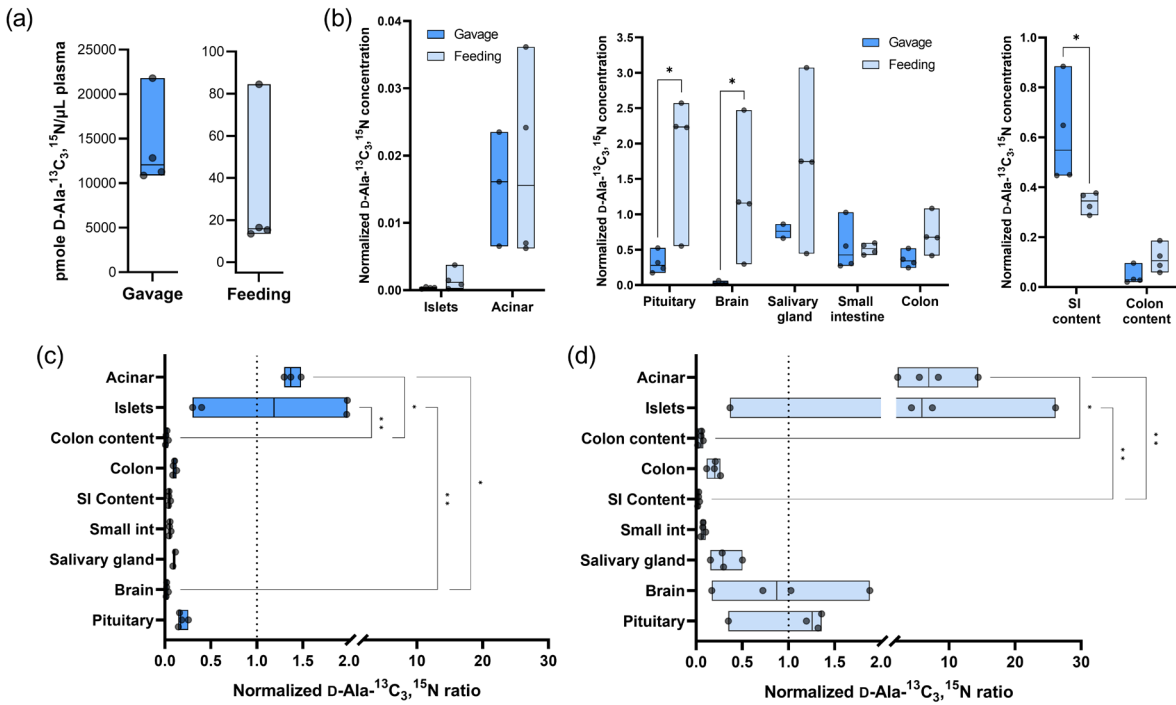


**Figure 3.** Biodistribution of orally administered D-Ala-<sup>13</sup>C<sub>3</sub>, <sup>15</sup>N in germ-free mice. (a) Concentrations (pmole/μL) of D-Ala-<sup>13</sup>C<sub>3</sub>, <sup>15</sup>N detected in plasma of animals orally administered with D-Ala-<sup>13</sup>C<sub>3</sub>, <sup>15</sup>N via gavage or feeding. (b) Normalized D-Ala-<sup>13</sup>C<sub>3</sub>, <sup>15</sup>N concentrations (Equation 2) in various sample types. Asterisks indicate statistical significance from Mann-Whitney tests. (c) (d) Normalized D-Ala-<sup>13</sup>C<sub>3</sub>, <sup>15</sup>N ratios (Equation 3) in various sample types in (c) gavage and (d) feeding experiments. Asterisks with brackets indicate statistically significant difference (p<0.05) between sample types from the post hoc Dunn's multiple comparison after Kruskal-Wallis ANOVA (\*\* p<0.01, \* p<0.05). Each data point represents one sample from one individual animal. Floating bars indicate minimum and maximum, and the middle lines indicate median. SI – small intestine.

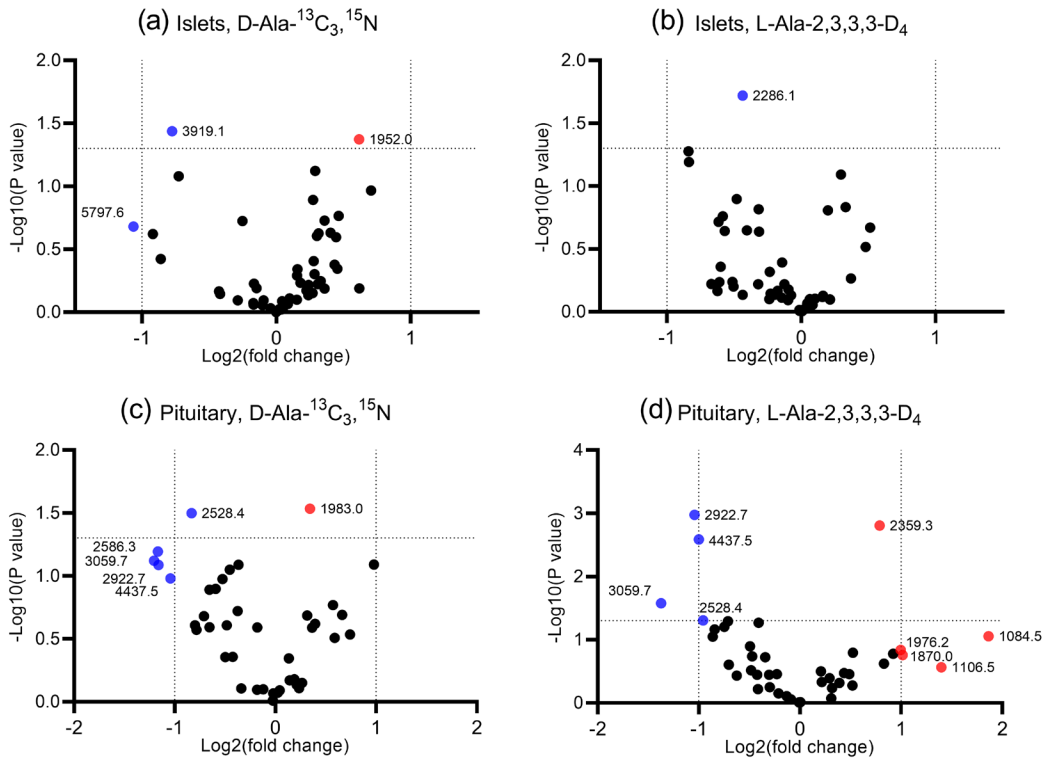


**Figure 4.** (a)(b) Pancreatic islets and (c)(d) pituitary gland peptide profile differences after 2-weeks of D-Ala-<sup>13</sup>C<sub>3</sub>, <sup>15</sup>N or L-Ala-2,3,3,3-D<sub>4</sub> treatment in drinking water compared to control (water only) (n=4). Volcano plots showed results of uncorrected multiple t-tests between treated and control groups. Each data points represents the fold change and p values of log2-transformed, normalized peak intensities in the samples from treated animals compared to control. Data points with larger than 2-fold absolute fold change and/or p values smaller than 0.05 are marked with observed m/z values and color coded (blue for decrease and red for increase in the treated group compared to control).

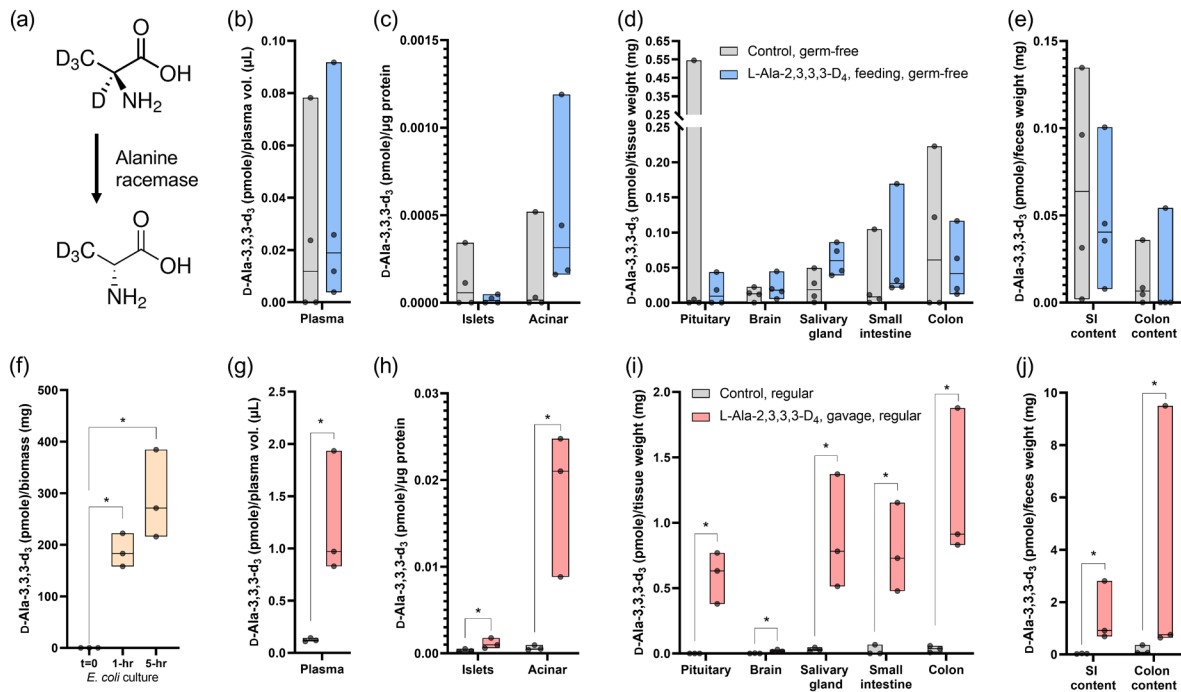


**Figure 5.** (a) Illustration of alanine racemase activity converting L-Ala-2,3,3,3-d<sub>4</sub> to D-Ala-3,3,3-d<sub>3</sub>. (b)(c)(d)(e) Concentrations of D-Ala-3,3,3-d<sub>3</sub> in samples from germ-free mice after two-week feeding of L-Ala-2,3,3,3-d<sub>4</sub> or regular water as control. (g)(h)(i)(j) Concentrations of D-Ala-3,3,3-d<sub>3</sub> in samples from regular mice 1-hour after gavage feeding of solution containing the same stable isotope labeled L-Ala or saline as control. Pairwise comparisons using Mann-Whitney tests (two-tailed for germ-free and one-tailed for regular mice) were performed between the control and dosed groups individually for each sample type. Asterisks with brackets indicates statistical significance ( $\alpha=0.05$ ). (f) Racemization of L-Ala-2,3,3,3-d<sub>4</sub> in bacterial culture. One-tailed Mann-Whitney tests were used to compare between time zero and the two other time points individually. Each data point represents one sample from one individual animal or one tube of bacterial biomass. Floating bars indicate minimum and maximum, and the middle lines indicate median. SI – small intestine.